CONCRETE LIBRARY OF JSCE NO.2, DECEMBER 1983

ULTIMATE STRENGTH OF REINFORCED CONCRETE FIXED SLAB SUBJECTED TO CONCENTRATED LOAD

(Reprint from Transaction of JSCE, No.315, Nov. 1981)

Hiroshi SEKI

SYNOPSIS

The experimental work regarding the ultimate strength of fixed slabs is initially carried out, including such variables as f_c', f_{sy}, ρ, d, cross sectional area of boundary beams and diameter of loading plate. Due to the testing results, the theoretical equation is derived taking into consideration the membrane effect, and practical equation of shear strength is proposed. Unbalanced forces, which are experimentally recognized in the section such as in-plane force, enhance the ultimate flexural strength and is more influenced in slabs with a higher value of $\rho f_{sy}/f_c'$ and larger restraints of lateral movement. The calculation equation regarding punching shear is induced in consideration of such items as critical section at shear failure, in-plane force acting as the cross section of slabs and influence of effective depth. Finally, the following practical equation for the shear strength of fixed slabs is recommended, in which β_d and β_N are the function of effective depth and that of rigidity, respectively.

$$\tau_u = \beta_0 (1 + \beta_d + \beta_N) f_{tu}$$

H. Seki is a professor of civil engineering at Waseda University, in Tokyo, Japan. He received his Doctor of Engineering Degree in 1978 from University of Tokyo. His main interests is now the theorem of long-term safety of reinforced concrete structures including cracking, deterioration and corrosion of reinforcing bars.

---

1. INTRODUCTION

Many experimental and theoretical research works have been so far carried out regarding simply supported slabs. At the present stage it is possible to calculate the ultimate strength of slabs with fairly good accuracy by way of either the yield line theory[1] applicable for the flexural strength or the equations for the punching shear proposed due to the experimental works.

On the other hand, few works have been done regarding fixed slabs. It might be reasoned that in-plane force occurred due to the restraints of slab boundaries complicates the analytical approach, the relationship between in-plane force and ultimate strength of slabs is not clear, and the quantitative analysis of the boundary restraints is difficult.

The reinforced concrete slabs, generally designed as fixed slabs, are main structural members of such port and harbour facilities as the upper element of piled wharves and the caissons of breakwaters. These members in most cases are subjected to concentrated load instead of uniform loads, and it is considered necessary to evaluate the collapse mechanism and the ultimate strength with regard to fixed slabs. The purpose of the present paper is to establish a practical and rational design method applicable to slabs under the real loading and supporting conditions according to the experimental and theoretical approach. Experimental work is in this paper limited to the square slabs without shear reinforcements.

2. REVIEW OF ULTIMATE STRENGTH REGARDING REINFORCED CONCRETE SLABS

2.1 Punching Failure

Flat slabs and footings tend to fail in punching shear because of large bending moment and shear force acting at the areas jointed with columns. Table 1 summarizes the main calculation equations of simply supported slabs deduced from the experimental works. Kinnunen[10] proposed the calculation method of shear strength based on the fracture model.

In-plane force effect was initially pointed out[11] from the fact that ultimate strength in flexure remarkably exceeded the load calculated by way of the yield line theory. Hewitt[12] separated in-plane force occurred at the slab boundary into the fixed boundary action and the compression membrane action. He assumed the failure model similar to the Kinnunen's model and proposed the iteration method of shear strength.

Table 1 Equations for punching shear of slab

Researcher	Proposed equation (Unit: N, mm)
Moe(2)	$P_{shear}=\dfrac{1.25\left(1-0.075\dfrac{a}{d}\right)bd\sqrt{\sigma_{cu}}}{1+0.435\dfrac{bd\sqrt{\sigma_{cu}}}{P_{flex}}}$ $P_{flex}=8\,m_u\left(\dfrac{1}{1-a/l}-3+2\sqrt{2}\right)$ (free of corner lifting) $=8\,m_u\dfrac{1}{1-a/l}$ (restrain of corner lifting) $m_u=\sigma_{cu}qd^2(1-q/2)$, $b=b_0$
Yitzhaki (3)	$P_{shear}=d^2\left(1-\dfrac{q}{2}\right)(8.24+1.31\,p\sigma_{sy})\left(1+0.5\dfrac{a}{d}\right)$
Herzog (4)	$P_{shear}=bd\sqrt{\sigma_{cu}}(0.212+0.0575\,p\sigma_{sy})$ $b=4(a+d)$, $p\sigma_{sy}\leqq 53.9$
Regan (5), (6)	$P_{shear}=0.300\,bd(84.9\,\sigma_{cu}p)^{0.4}$ $b=b_0+3.5\,\pi d$
Kakuta etc (7)	$P_{shear}=\dfrac{0.211\,bd\sqrt{\sigma_{cu}}\left(1+1.60\dfrac{p\sigma_{sy}}{\sqrt{\sigma_{cu}}}\right)}{1+\dfrac{d}{200}}$ $b=b_0+3\,\pi d$. $p\sigma_{sy}/\sqrt{\sigma_{cu}}\leqq 1.04$
Long (8), (9)	Lower value among the following two equations $P_{shear}=\dfrac{\sigma_{sy}pd^2(1-0.59\,q)}{0.2-0.9\dfrac{a}{l}}$ (flexural type) $P_{shear}=\dfrac{0.416\,bd(100\,p)^{0.25}\sqrt{\sigma_{cu}}}{0.75+4\dfrac{a}{l}}$ (shear type) $b=4(a+d)$

2.2 Flexural Failure

The yield line theory is mostly applicable to calculate the flexural strength of reinforced concrete slabs. The ultimate strength of slabs subjected to concentrated load varies with such factors as the yield line pattern and the ratio of $2r/\ell$, if the yield line theory is introduced. Even if square slab is assumed to be circular slab, the difference of the ultimate strength tends to be minor in the region that $2r/\ell$ is 0.05 to 0.30. Therefore, the flexural strength is in this paper calculated with the following equation.

$$P_{flex2} = \frac{2\pi m_u (1 + i)}{1 - \frac{2r}{\ell}}$$

3. LOADING METHODS AND TESTING RESULTS

3.1 Testing Procedures

Main factors which affect the punching shear strength of slabs might be properties of structural materials, dimensions of slabs, supported conditions, loading conditions and amount of shear reinforcement. In this paper, the slabs and the testing conditions are limited because port facilities are in consideration. The proto-type specimens adopted are square slabs restrained with the supporting concrete beams along the boundary. Main variables consist of strength of concrete (f_c' = 24 to 40 MP_a), yield point of reinforcements (f_{sy} = 293 to 409 MP_a), depth of slab (d = 0.043 to 0.161 m), reinforcement ratio (ρ = 0.72 to 2.06%), degree of restraints at boundary (cross-section of boundary beams (0.20 x 0.26 to 0.60 x 0.38 m)), and area of concentrated load (mainly, ϕ0.05 to ϕ0.30 m). Table 2 indicates the dimensions of specimens and the testing conditions. Square slabs have 1.0 x 1.0 m. Boundary beams of fixed slabs are jointed with the testing bed by way of nuts. The items of measurements are strain, deflection, deformation of boundary beams, cracking and failure load. Strain and deflection at slab element are measured at the direction of both the center lines of slabs and the diagonal lines of slabs. Data of vertical and lateral movement of boundary beams are obtained. Fig. 1 illustrates the loading test.

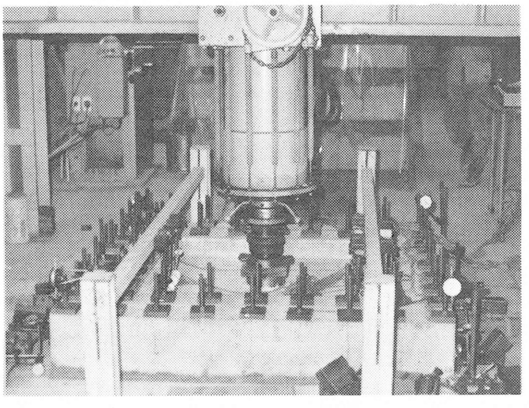

Fig. 1 Loading apparatus

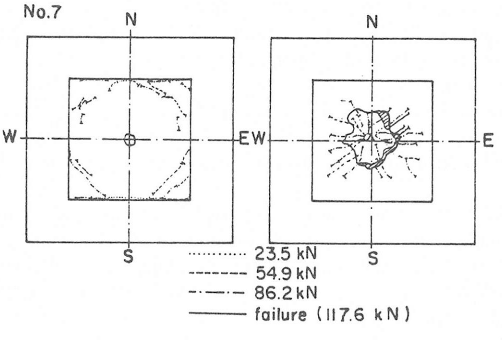

Fig. 2 Crack pattern

3.2 Cracking

a) Crack pattern

Fig. 2 shows the crack pattern. Though slabs failed in shear have incomplete flexural crack pattern, the yield pattern of slabs failed in flexure (specimen No. 17 and No. 18) is similar to the shape of circular or octagon inscribed in a square slab.

b) Crack width

Lower surface of slab has larger crack width compared with upper surface. Average crack width (average of larger three data) is 0.7 to 1.0 times as large as maximum crack width, and is less than 0.15 to 0.20 mm at half of shear failure load. In this case, then, there is no concern to confine crack width from the point of durability[13].

Table 2 Test conditions

No. of specimen	Loading condition (mm)	Dimension of specimen				Properties of materials		
		Slab			Boundary beam (width × height) (mm)	Comp. strength of concrete (N/mm^2)	Reinforcement	
		Effective depth (mm)	Bar arrangement				Yield point (N/mm^2)	Elongation (%)
			Main bar	Reinforcement ratio (%)				
1	ϕ 50	48	ϕ 6, @6	0.99	350×260	31	335	31
2		47	ϕ 6, @6	1.01	350×260	39	293	26
3	ϕ 100	45	ϕ 6, @6	1.05	350×260	24	362	30
4		48	ϕ 6, @6	0.99	350×260	28	335	31
5		47	ϕ 6, @6	1.01	350×260	29	394	24
6		44	ϕ 6, @6	1.08	350×260	38	293	26
7		45	ϕ 6, @6	1.05	350×260	38	293	26
8		43	ϕ 6, @6	1.10	350×260	39	293	26
9		44	ϕ 6, @9	0.72	350×260	30	409	16
10		46	ϕ 6, @3	2.06	350×260	30	409	16
11		45	ϕ 6, @6	1.05	200×260	30	409	16
12		47	ϕ 6, @6	1.01	600×260	29	409	16
13		53	ϕ 6, @6	0.89	350×260	33	293	26
14		71	ϕ 9, @9	1.00	600×290	27	367	30
15		103	ϕ 9, @6	1.03	600×320	29	367	30
16		161	ϕ 13,@9	0.92	600×380	28	415	20
17	ϕ 190	41	ϕ 6, @6	1.16	350×260	31	293	26
18	ϕ 300	45	ϕ 6, @6	1.05	350×260	31	293	26
19	Unifom load	45	ϕ 6, @6	1.05	350×260	25	362	30
20		46	ϕ 6, @6	1.03	350×260	29	293	26
21		44	ϕ 6, @6	1.08	350×260	39	362	30
22		45	ϕ 6, @6	1.05	200×260	28	409	16
23		45	ϕ 6, @6	1.05	600×260	27	409	16
24	ϕ 100	43	ϕ 6, @6	1.10	350×260	39	293	26
25	Unifom load	45	ϕ 6, @6	1.05	350×260	36	293	26
26	ϕ 100	45	ϕ 6, @6	1.05	—	33	293	26

Note:
1. Dimension of slab element 1,000 x 1,000 mm
2. Supporting conditions are fixed slabs for No. 1 to No. 25 and simply supported slab for No. 26, respectively.
3. Uniform load means the sixteen points' loading.

3.3 Deformation of Boundary Beams and Slabs

No vertical deformation of boundary beams occurred with the limits of measured accuracy. Larger lateral movement toward outward direction is observed in smaller boundary beams. Lateral deformation tends to increase in accordance with increase of applied load, as might show the occurrence of in-plane force in slab area.

After cracking, the deflection calculated with the elastic analysis does not agree with that measured. The change of flexural rigidity (denoted as k) is defined for the slabs failed in flexure as follows, in which k is considered to be the ratio of δ_c (calculated deflection of circular elastic slab) and δ_{mea} (measured).

$$k = s \frac{P}{\delta_{mea}}$$

where

$$s = \frac{12\,(1-\nu^2)}{4\pi E h^3}\left(\frac{r^2}{4}\log\frac{2r}{\ell} - \frac{3r^2}{16} + \frac{\ell^2}{16}\right)$$

At the failure stage, k is 0.146 for specimen No. 17 and 0.143 for specimen No. 18, respectively.

Fig. 3 shows the strains of slab center-line both at upper surface and at lower surface where no crack is observed. These strains do not coincide with the value calculated with the elastic analysis. The axial stress at center line of slab, which is obtained from strain at center line and strain perpendicular to center line, is also indicated in the figure. It is likely from the figure that in-plane force occurs even at the lower stage of loading and increases in accordance with increase of applied load, this phenomenon being similar to the test results of boundary beams.

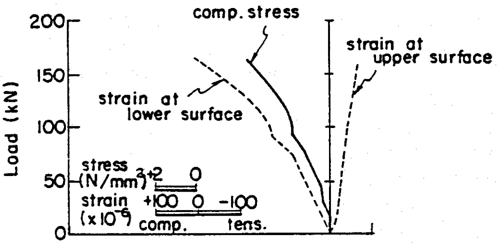

Specimen No.14 (270mm from slab center)

Fig. 3 Measured strain and calculated axial stress at slab surface

3.4 Punching Shear Failure

a) Fracture pattern

Three fracture patterns are observed in the loading test, such as the flexural failure, the shear failure at the joint between slab and boundary beam, and the punching shear failure near the loading plate. Specimens, in which the diameter of loading plate is over 19 cm, fail in flexure. Specimens loaded at 16 points are suddenly pushed down at slab area from boundary beams.

In most specimens, the center upper part of slab area is punched at the diameter of loading plate, when crack pattern is incomplete and no sign of failure is observed beforehand. The inclined angle of the truncated cone measured after loading test ranges from 25° to 30°. As the inclined crack occurs at the neutral axis of cross-section of members[2], it is considered the critical section is in the region of 0.71d to 1.07d from the loading plate. In this paper, the critical section is defined at 1.0d from the loading plate.

b) Testing variables and shear strength

Index $\rho \times f_{sy}$ is adopted as the influential factor of reinforcement because of Kakuta's research results[7]. It is likely that final shear failure occurs nearly at the flexural failure stage for flexure type of Long's equation and for lower $\rho \times f_{sy}$ of Moe's equation shown in Table 1. In fixed slabs tested, no clear influence of index $\rho \times f_{sy}$ is observed.

Tensile strength of concrete expresses with more accuracy the shear failure of slabs instead of compressive strength of concrete[7], as might be reasoned that the final failure mechanism is similar to diagonal tension. In this paper, tensile strength is calculated from the equation $f_{tu} = 0.438 \sqrt{f_c'}$. Test results show that the effect of f_{tu} toward punching shear is not evident because of the limited range of concrete strength.

Moe indicated the area of loading and the effective depth of slab as the index of a/d. However the index a/d is not adequate, as is shown by Kakuta[7], to express two factors simultaneously. Test results in this paper are mainly arranged with effective depth of slab, this method being similar to the research work of Kakuta[7], Kani[14] and Kennedy[15]. As is shown in Fig. 4, shear strength of fixed slabs decreases in accordance with increase of effective depth.

3.5 Comparison with Present Design Methods

Design shear strength is calculated with such codes as Reinforced Concrete Code of JSCE (1980), CP-110 (The structural use of concrete, 1972) and CEB-FIP Model Code (1977). Table 3 shows the calculated results in which the ratio of the failure punching load and the calculated load varies in wide range. On the contrary, the specimen No. 26 and Kakuta's slabs[7], which are simply supported slabs, have the lower ratio by 1.0 to 1.5 compared to the fixed slabs tested in this paper. Though the failure load in punching shear is in excess of the calculated results based on the present codes, it is likely that the design load of fixed slab tends to be underestimated compared to that of simply supported slabs.

Table 3 also indicates the calculated results based on the proposed equations. The ratio of the failure load and the calculated load ranges from 1.6 to 3.0, precluding such cases that specimen has larger effective depth (No. 16) and Hewitt's equation is applied with the restraint factor Fr = 0.5 to 1.0. All proposed equations except Hewitt's are deduced based on the experimental and research work of the simply supported slabs.

Therefore, there remain some problems in adopting the present design methods. It is considered that this discrepancy comes from the effect of in-plane force which is attributed to the horizontal restraints of boundary beams. This phenomenon is partially estimated from Hewitt's equation, in which the failure load depends on the boundary restraint.

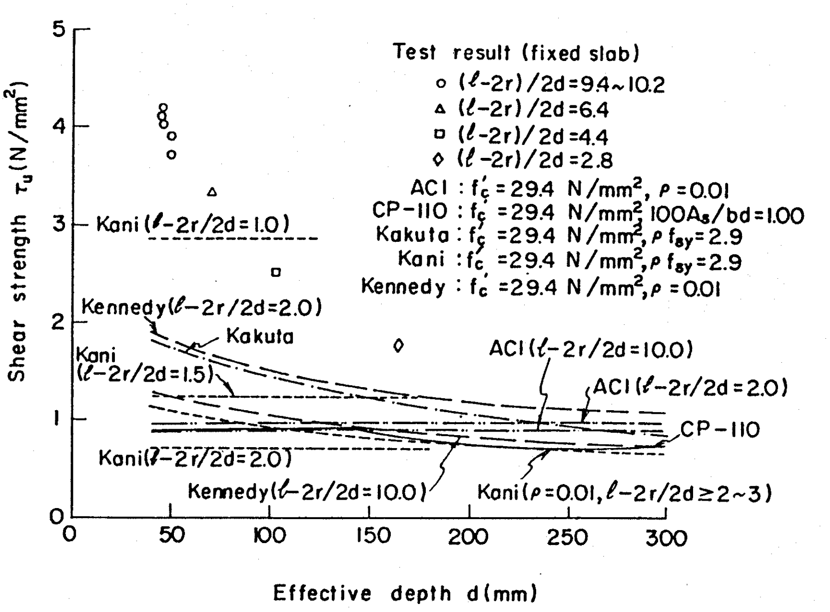

Fig. 4 Influence of effective depth toward shear strength of slab

Table 3 Comparison between testing results and calculation values regarding punching shear

No. of Specimen	Failure load P_{test} (kN)	$\frac{P_{test}}{P_{RC}}$	$\frac{P_{test}}{P_{ACI}}$	$\frac{P_{test}}{P_{CP}}$	$\frac{P_{test}}{P_{CEB-FIP}}$	P_{test}/P_{cal}									
						Moe	Yitzhaki	Herzog	Regan	Kakuta	Long	Hewitt			
												F_r=0.00	F_r=0.50	F_r=0.75	F_r=1.00
1	8.0	4.65	3.38	2.58	4.22	1.91	2.03	2.33	2.16	1.45	2.09	2.72	1.00	0.76	——
2	9.6	5.23	3.70	2.96	4.20	2.16	2.58	2.68	2.42	1.77	2.48	3.30	1.04	——	——
3	10.8	5.27	3.73	3.35	4.71	1.84	2.29	2.40	2.84	1.69	2.66	3.70	1.64	1.27	1.04
4	13.0	5.84	3.80	3.47	4.81	1.96	2.57	2.62	2.96	1.92	2.75	3.88	1.60	1.23	1.02
5	9.5	4.39	2.83	2.60	3.49	1.40	1.83	1.78	2.20	1.31	2.04	2.74	1.18	0.90	0.74
6	10.4	4.70	2.96	2.87	3.71	1.62	2.35	2.08	2.35	1.64	2.26	3.40	1.20	0.93	——
7	12.0	5.27	3.30	3.23	4.22	1.81	2.64	2.35	2.63	1.86	2.56	3.79	1.33	1.02	——
8	9.5	4.02	2.72	2.70	3.38	1.49	2.20	1.90	2.17	1.52	2.12	3.18	1.10	0.85	——
9	10.4	4.70	3.29	3.58	4.43	1.78	2.42	2.39	3.01	1.80	2.58	4.16	1.46	1.11	——
10	12.0	5.13	3.58	2.63	3.26	1.58	1.81	1.93	2.12	1.36	2.16	2.79	1.27	1.00	0.84
11	9.0	3.95	2.77	2.59	2.98	1.36	1.81	1.68	2.16	1.25	1.98	2.85	1.16	0.88	0.72
12	10.0	4.62	2.99	2.73	3.67	1.47	1.91	1.85	2.33	1.35	2.16	3.01	1.25	0.95	0.78
13	9.6	3.41	2.27	2.29	2.86	1.26	1.72	1.73	1.82	1.32	1.74	2.46	0.93	0.72	——
14	18.0	4.72	3.14	2.54	3.94	1.61	1.85	2.06	2.15	1.47	2.27	1.97	0.98	0.78	0.65
15	25.0	3.87	2.47	1.91	3.11	1.38	1.36	1.60	1.51	1.17	1.77	1.12	0.64	0.53	0.45
16	37.4	2.89	1.88	1.38	2.58	1.26	0.92	1.21	1.07	0.94	1.39	0.80	0.46	0.38	0.32
24	10.5	4.44	3.01	2.98	3.37	1.66	2.44	2.10	2.40	1.68	2.35	3.52	1.22	0.94	——
Average		4.54	3.05	2.73	3.70	1.62	2.04	2.04	2.25	1.50	2.20	2.91	1.14	0.89	0.73

4. ESTINATION OF SHEAR CAPACITY IN FIXED SLABS

4.1 In-plane Force

It is considered that the neutral axis of a slab section is determined from the geometrical deformation of bent strip rather than the equilibrium of distributed stress in the section, providing that free deformation at the slab boundary is restrained. Then the unbalanced forces exist in the section such as in-plane force.

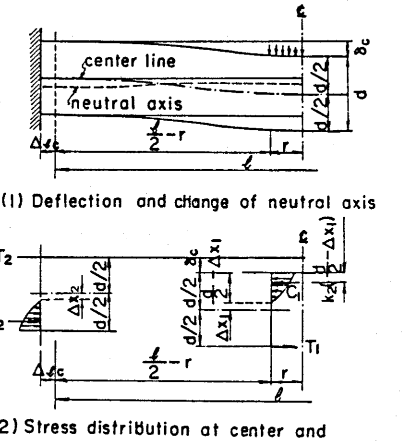

(1) Deflection and change of neutral axis

(2) Stress distribution at center and at boundary

Fig. 5 Deformation and stress distribution of slab

Though the shape of the neutral axis can not be easily decided at the flexural ultimate stage, the distance of the neutral axis (Δx) from the center line of slab ($d/2$) might be the functions of the deflection of slab and the rigidity of boundary beams. Fig. 5 indicates the idea explained above. In this chapter, circular slab is examined instead of square one because that the final failure pattern is similar to the circular shape, as is mentioned in 2.2 and 3.2, and the stress state near the concentrated load is nearly equal to that of circular slab.

4.2 Analysis of Flexural Capacity

a) Equation of flexural capacity

It is assumed that the stress distributions and the distances moved from the neutral axis (Δx_1 and Δx_2) are those shown in Fig. 5(b) at the center slab and at the circumference of slab, respectively.

(i) Relation between in-plane force and Δx: The force acted at unit width of slab center area might be written as follows.

$$C_1 = k_3 f_{co}' k_1 (\frac{d}{2} - \Delta x_1) \tag{1}$$

$$T_1 = f_{sy} \rho d \tag{2}$$

$$F_1 = C_1 - T_1 \tag{3}$$

k_3 expresses the ratio between concrete strength of members and that of specimens, and k_1 means the ratio between maximum compressive stress and average compressive stress. It is likely that k_1 is 0.7 to 0.9 and k_3 is 0.85 to 1.0, respectively. The value of 0.85 is adopted in this paper. f_{co}' is the compressive strength at the bi-axial stress state, and is defined as $f_{co}' = 1.11 f_c'$[16]. Eq. (1) and (2) are substituted into Eq. (3), and in-plane force of slab center area F_1 is expressed as follows.

$$F_1 = -0.8 f_c' \Delta x_1 + A \tag{4}$$

where

$$A = 0.40d f_c' - f_{sy} \rho d$$

Unit in-plane force acting at the boundary of slab, denoted as w, is derived with the similar manner.

$$w = -0.8 f_c' \Delta x_2 + A \tag{5}$$

(ii) Relation between in-plane force and lateral movement at boundary: As in-plane force acting at the circular slab is w shown in Fig. 6, unit forces acting at boundary beams (denoted as w_x and w_y) are written as $w_x = w \cos^3\theta$ and $w_y = w \sin\theta \cos^2\theta$, respectively. Then, the total force W_x and W_y at half span of boundary beams comes to $W_x = \sqrt{2}\, w\ell/4$ and $W_y = (2 - \sqrt{2})\, w\ell/4$. It is considered because of simplification that uniform load $\sqrt{2}\, w/2$ acts to boundary beams instead of w_x. The lateral movement at the center span of boundary beams is expressed as follows;

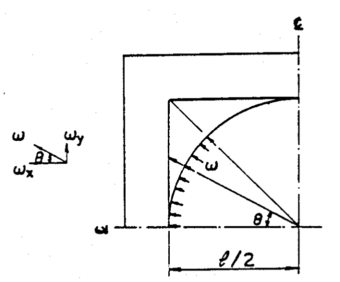

Fig. 6 Force acting at boundary beam

$$\Delta\ell_c = Kw$$

where

K: coefficient of flexural rigidity

$$K = \frac{\sqrt{2}\ell^4}{768EI} + \frac{3\sqrt{2}\ell^2}{32A_oG}$$

(iii) Relation between in-plane force at slab center area and that at slab boundary: If the fan-shaped slab element, in which radius is r and ($\ell/2 - r$)

and angle is $d\theta$, is considered, rF_1 does not equal to $\ell w/2$ though F_1 acting at radius r and w at radius $(\ell/2 - r)$. This might be reasoned that in-plane force w' also occurs at the circumference direction of slab. It is however difficult to analyze the value and distribution of w'. On the assumption that w' is average of F_1 and w, the following relation is derived.

$$F_1 = w \tag{6}$$

(iv) Relation between ultimate moment (m_u) and Δx: If m_u is defined at the plastic centroid of cross section, ultimate moment at slab center area m_{u1} is written as follows using the signs of Fig. 7,

$$m_{u1} = C_1 \{g - k_2 (\frac{d}{2} - \Delta x_1)\} + T_1 (d - g)$$

Eq. (1), (2) and $k_2 = 0.85/2$ are substituted into the above equation.

$$m_{u1} = -0.34 f_c' \Delta x_1^2 - B\Delta x_1 + C$$

where

$$B = (0.8 g - 0.34 d) f_c'$$

$$C = 0.40 d f_c' (g - 0.212 d) + f_{sy} \rho d (d - g)$$

$$g = \frac{0.425 h + d q_t}{0.85 + q_t}, \quad q_t = \frac{\rho_t f_{sy}}{1.11 f_c'}, \quad \rho_t = \rho\frac{d}{h}$$

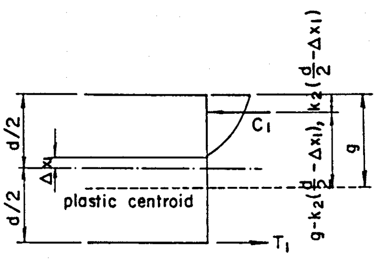

Fig. 7 Cross-section of slab

Similarly at slab boundary,

$$m_{u2} = -0.34 f_c' \Delta x_2^2 - B\Delta x_2 + C$$

(v) Relation between flexural capacity (P_{flex1}) and ultimate moment (m_u): If the ultimate moments at the circumference of slab are m_{u1} at slab center area and m_{u2} at slab boundary, the flexural capacity P_{flex1} can be calculated by way of the yield line theory.

$$P_{flex1} \fallingdotseq \frac{2\pi}{\ell - 2r} \{(r + \frac{\ell}{2}) m_{u1} + (\frac{3\ell}{2} - r) m_{u2}\}$$

(vi) Relation between flexural capacity (P_{flex1}) and deflection (δ_c): The central deflection of circular slab inscribed in a square slab is written as follows,

$$\delta_c = \frac{s}{k} P_{flex1}$$

where

$$s = \frac{12 (1 - \nu^2)}{4 \pi E h^3} \{\frac{r^2}{4} \log \frac{2r}{\ell} - \frac{3r^2}{16} + \frac{\ell^2}{16}\}$$

k = 1 means the elastic solution. The reinforced concrete slab has actually the coefficient k less than 1, and it is assumed that k nearly equals 0.15 based on the result of 3.3. Then

$$P_{flex1} = \frac{0.15}{s} \delta_c$$

(vii) Δx, lateral movement ($\Delta \ell_c$) and deflection (δ_c): The relation of three values Δx, $\Delta \ell_c$ and δ_c can be induced in consideration of the geometrical condition of the neutral axis. As it is difficult to make clear the shape of neutral axis line in the slab element, the experimental approach is adopted in this paper. It might be considered that Δx_1 increases in accordance with the increase of $\Delta \ell_c$ and δ_c and the increasing ratio of $\Delta x_1/\Delta \ell_c$ decreases in accordance with the increase of $\delta_c/(\ell - 2r)$. Then it might be possible due to the quantitative consideration to express Δx_1 as follows.

$$\Delta x_1 = \alpha \frac{\ell - 2r}{\delta_c} \Delta \ell_c + \beta \delta_c + \gamma \tag{7}$$

When $\Delta \ell_c$ equals zero, that is, completely fixed slab, neutral axis line does not alter. In this case, the sum of Δx_1 and Δx_2 coincides with δ_c. Due to this relation and the equations (4) to (6), β comes to 1/2 and γ to zero, respectively. Then the equation (7) can be rewritten as follows.

$$\Delta x_1 = \alpha \frac{\ell - 2r}{\delta_c} \Delta \ell_c + \frac{\delta_c}{2}$$

(viii) Summary: The following simultaneous equations are derived from (i) to (vii).

$$w = -0.80\, f_c'\, \Delta x_1 + A, \qquad w = \frac{\Delta \ell_c}{K}$$

$$P_{flex1} = \frac{4\pi \ell m_u}{\ell - 2r}, \qquad P_{flex1} = \frac{0.15}{s}\,\delta_c$$

$$m_{u1} = -0.34\, f_c'\, \Delta x_1^2 - B \Delta x_1 + C$$

$$\Delta x_1 = \alpha \frac{\ell - 2r}{\delta_c} \Delta \ell_c + \frac{\delta_c}{2}$$

If properties of materials and dimensions of slabs are known, we can obtain the unknown (w, Δx_1, $\Delta \ell_c$, m_{u1}, δ_c, P_{flex1}) by determining the factor α.

b) Flexural capacity of fixed slab

It is necessary to determine the factor α with higher accuracy based on larger number of data in which slabs fail in flexure. α is approximately 3.0 due to the test results of specimens No. 17 and No. 18, though lower accuracy. Table 4 indicates the ratio of the testing failure load (P_{test}) and the loads which are calculated with yield line theory (P_{flex2}) and with the proposed method (P_{flex1}) including in-plane force. P_{flex1}/P_{flex2} ranges 1.5 to 1.7.

Strain and deformation of boundary beams are shown in Fig. 8. In-plane forces acting toward the beams are 129 N/mm for No. 17 and 168 N/mm for No. 18, respectively, by solving the simultaneous equations of a). Though the calculated value more or less exceeds the measured value, it might be possible to estimate the deformation of boundary beams.

4.3 Analysis of Shear Capacity

It might be difficult to analyze the failure phenomenon of punching shear strictly. Then, the following assumptions are in consideration so as to obtain shear capacity.

Table 4 Comparison of ultimate capacity and shear strength between experimental results and calculation values

No. of Specimen	Ultimate strength			Shear strength
	$\frac{P_{shear2}}{P_{flex1}}$	$\frac{P_{test}}{P_{shear2}}$	$\frac{P_{test}}{P_{flex1}}$	$\frac{\tau_{test}}{\tau_2}$
1	0.51	1.03	(0.52)	1.01
2	0.58	1.06	(0.61)	1.16
3	0.64	1.29	(0.82)	1.30
4	0.68	1.22	(0.83)	1.35
5	0.62	0.97	(0.59)	1.00
6	0.83	0.86	(0.71)	1.02
7	0.83	0.97	(0.81)	1.15
8	0.85	0.77	(0.66)	0.93
9	0.84	1.00	(0.84)	1.14
10	0.34	1.62	(0.55)	1.25
11	0.63	1.07	(0.67)	0.99
12	0.59	0.98	(0.58)	1.05
13	0.73	0.70	(0.51)	0.83
14	0.40	1.20	(0.48)	1.24
15	0.29	1.08	(0.31)	1.10
16	0.20	0.99	(0.20)	0.98
17	1.26	(0.78)	0.98	——
18	1.57	(0.64)	1.01	——
24	0.86	0.87	(0.75)	0.85

Note: ① Failure pattern is
No. 1~No. 16, No. 24 punching shear failure
No. 17, No. 18 flexural failure
② Regarding the specimens failed in flexure
No. 17, P_{flex1}=129 kN, P_{flex2}=84 kN, P_{test}=126 kN,
No. 18, P_{flex1}=178 kN, P_{flex2}=107 kN, P_{test}=180 kN
③ $\tau_2 = \beta_0(1+\beta_d+\beta_N) f_{tu}$

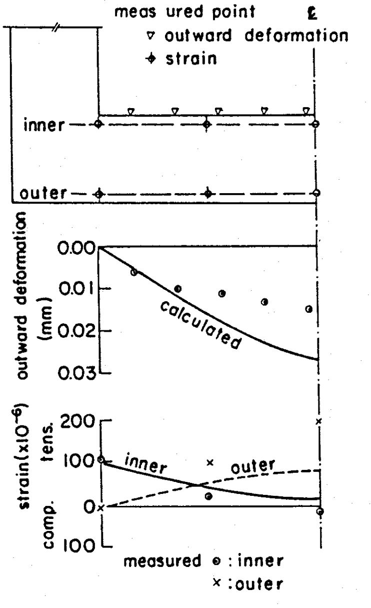

Specimen No.18

Fig. 8 Calculated and measured data of boundary beam

The cirtical section is at the distance of d from the circumference of loading plate based on the consideration of 3.4. In-plane force is in proportion to the applying load. Tensile strength of concrete is written as 1.11 x 0.438 $\sqrt{f_c'}$ because of the bi-axial stress state of slabs. The dowel action due to the tensile reinforcement enhances the shear capacity by 20 percents, as was assumed by Hewitt[12].

Regarding the shear strength acted with the axial force, the equations of ACI 318-77 and Mattock can not estimate the shear capacity toward the fixed slab. Following equation is adopted in this paper.

$$\tau = f_{tu}\sqrt{1 + \frac{f_n}{f_{tu}}} \qquad (8)$$

where f_n: average axial stress

Due to the assumptions of critical section and dowel action, τ can be written as $\tau = P_{shear1}/2.4\,\pi d\,(r + d)$. Equation (8) is rearranged by substituting f_n and f_{tu} into (8), as follows.

$$P_{shear1} = \frac{Q}{2} \{QR + \sqrt{(QR)^2 + 4}\}$$

where

$$Q = 3.70 \pi d (r + d) \sqrt{f_c'}$$

$$R = \frac{w}{1.54 \, d \, P_{flex1} \sqrt{f_c'}}$$

The method above mentioned does not include the influence of effective depth. Regarding reinforced concrete beams, Kani[14] and Kennedy[15] considered the shear strength as the function of $1/(d/10)^{0.25}$ and $1/(d/10)^{0.28}$, respectively. If shear failure in slabs is similar to that in beams, shear strength of slabs might be expressed as the function of effective depth of slabs, approximately likely $(d/10)^{0.25}$. This idea has been recognized in CP-110 and Kakuta[7]. When R_d is defined as the coefficient regarding the influence of the effective depth, that is, $P_{shear2} = P_{shear1} \cdot R_d$, the equation $R_d = 1/(2.0\ (d/10)^{0.25} - 1.7)$ is derived based on the experimental results. Table 4 indicates the calculation results. Specimens failed in shear have the failure load (P_{test}) lower than the calculated flexural load (P_{flex1}). The ratio of P_{shear2} to P_{flex1} ranges 0.20 to 0.86 precluding No. 17 and No. 18, as means that slab fails in shear before the flexural ultimate stage.

4.4 Relation between Flexural Capacity and Shear Capacity

Behavior of slabs, for which flexural failure precedes to shear failure, is examined in this section. From the calculation result, it is confirmed that the flexural capacity and the in-plane force increase in accordance with the decrease of K/10s (that is, the increase of rigidity of boundary beams) under the constant conditions of loading, materials and dimensions of slabs.

In-plane force is mainly varied with such factors as f_c', ρf_{sy} and K/10s, and d and 2r have small influence towards in-plane force. Fig. 9 shows the relation between $\rho f_{sy}/f_c'$ and P_{flex1}/P_{flex2}. It is likely that P_{flex1}/P_{flex2} increases considerably in accordance with decrease of $\rho f_{sy}/f_c'$ when boundary beams have large dimensions.

Furthermore, the results calculated under the variable combinations of loading, properties of materials and dimensions of slabs show as follows. It is inclined that failure pattern of slab transfer from flexure to shear providing that slab span increases under the constant value of d/ℓ and 2r/ℓ. This might be reasoned that shear strength decreases because of the increase of effective depth.

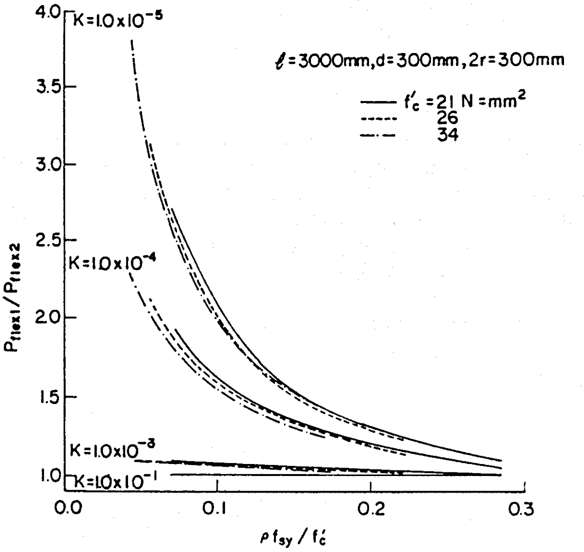

Fig. 9 Relationship between $\rho f_{sy}/f_c'$ and membrane effect

P_{shear2}/P_{flex1} naturally increases when the diameter of the loading plate increases under the constant condition of slab span. It is also shown that P_{shear2}/P_{flex1} becomes lower if the effective depth of slab, ρf_{sy} and the rigidity of boundary beams increase. f_c' shows little influence toward P_{shear2}/P_{flex1}.

4.5 Shear Strength of Fixed Slab

Shear strength is expressed as the summation of various factors in the literatures of [17] and [18]. The idea is applied to the fixed slab so as to recommend a practical equation, following.

$$\frac{\tau_u}{f_{tu}} = \beta_o \ (1 + \beta_{\rho f} + \beta_f + \beta_d + \beta_N) \qquad (9)$$

where $f_{tu} = 0.438 \sqrt{f_c'}$

$\beta_{\rho f}$: coefficient indicating the influence of reinforcing bar. $\beta_{\rho f} = 0$ at $\rho f_{sy} = 30$

β_f : coefficient indicating the influence of concrete compressive strength, $\beta_f = 0$ at $f_c' = 23.5$ N/mm^2

β_d : coefficient indicating the influence of effective depth, $\beta_d = 0$ at $d = 300$ mm

β_N : coefficient indicating the influence of in-plane force

τ_u : $P_{shear2}/2\pi\,(r + d)$

(i) β_o: The standard slab is as follows, $f_c' = 23.5$ N/mm^2, $\rho f_{sy} = 2.94$, $\ell = 3.0 \times 10^3$ mm, $d = 300$ mm, $2r = 300$ mm and $K = 1.0 \times 10^{-4}$ $(K/10s = 229)$. The calculation leads to the value of $\beta_o = 0.469$. Equation (9) does not, however, consider the factors $(\ell - 2r)/2\,d$ and ℓ. β_o tends to slightly decrease in accordance with the increase of $(\ell - 2r)/2\,d$, as is similar to the equation proposed by Kennedy. Larger the span ℓ, large the coefficient β_o under the condition of the same $(\ell - 2r)/2\,d$. However, β_o change slightly in the range of $d/\ell = 0.04$ to 0.12 and $2r/\ell = 0.05$ to 0.30. Then, β_o is determined as 0.47 in this paper.

(ii) $\beta_{\rho f}$ and β_f: $\beta_{\rho f}$ is nearly zero in the range of $\rho f_{sy} = 2.9$ to 5.9, as coincides with the experimental result of 3.4. β_f is also defermined as zero because the variation of β_f is limited to -0.01 to 0.02.

(iii) β_d: The relation between effective depth and β_d, shown in Fig. 10, is as follows.

$$\beta_d = \frac{3.0}{2.0(d/10)^{0.25} - 1.7} - 1$$

(iv) β_N: It might be possible to express β_N as the function of K/10s, as is shown in Fig. 11. β_N becomes constant in the case of larger value of K/10s, and this is caused by the fact that larger value of K diminishes the effect of in-plane force. When β_N is assumed as zero at K/10s = 230, it is likely that β_N is written as the following hyperbola.

$$\beta_N = \frac{230 - K/10s}{20\ (20 + K/10s)}$$

Equation (9) is rearranged due to the above consideration.

$$\frac{\tau_u}{f_{tu}} = \beta_o \; (1 + \beta_d + \beta_N)$$

τ_{test}/τ_2 in Table 4 means the calculation results based on the equation above mentioned. It is likely that shear strength of fiexed slab can be roughly estimated by way of this approach.

5. CONCLUSION

The experimental and theoretical work is carried out with regard mostly to the reinforced concrete fixed slabs (1.0 x 1.0 m) which are mainly subjected to concentrated load at the center of specimens. The calculation method of ultimate load and shear strength is proposed in consideration of in-plane force. The following conclusions are obtained within the limits of this study.

(1) Testing results obtained are as follows.

a) The observed crack widths range less than 0.2 mm even at the stage when the ratio of the applied load to the ultimate punching load comes up to around 50 percent.

b) In many cases failure occurs by punching along a truncated cone around a concentrated load. The angle of inclination from the circumference of loading plate ranges from 25 to 30 degrees. When the area of loading plate becomes larger, the collapse mode of slabs changes from punching shear to flexure.

c) It is confirmed that compressive in-plane force is generated at the early stage of loading and increases as the applied load increases.

d) The testing punching load is compared with the design codes and the proposed equations. Though the failure load in punching shear is in excess of calculated results, it is likely that the loads, based on the codes and the equations, tend to be underestimated.

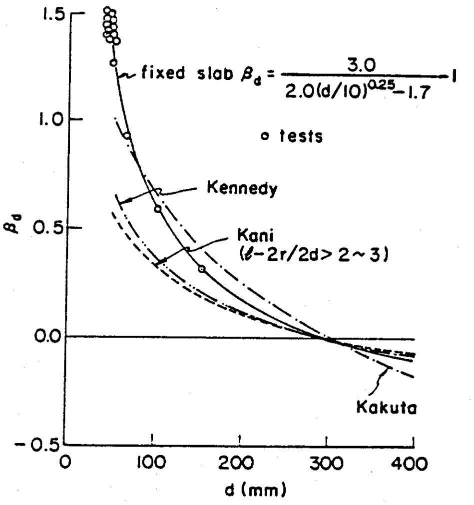

Fig. 10 Relationship between β_d and effective depth

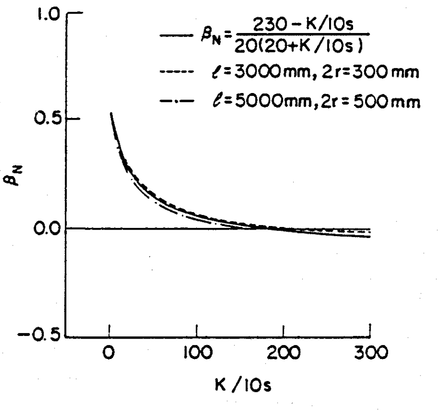

Fig. 11 Relationship between β_N and rigidity

(2) The calculation equation for flexural capacity is derived in consideration of in-plane force. The calculation results obtained according to that analysis are roughly in agreement with the testing results, such as deformation of boundary beams. In-plane force is more effected in slabs with a lower value of $\rho f_{sy}/f_c'$ and larger restraints of lateral movement.

(3) The calculation equation regarding punching shear is proposed in consideration of in-plane force. Two equations for flexure and shear can define

the boundary line by which the fixed slab will collapse.

(4) Finally, a practical equation for the shear strength of fixed slabs is recommended, as follows.

$$\tau_u = \beta_o \ (1 + \beta_d + \beta_N) \ f_{tu}$$

where

$$\beta_o = 0.47, \ f_{tu} = 0.438 \sqrt{f_c'}, \ \beta_d = \frac{3.0}{2.0(d/10)^{0.25} - 1.7} - 1$$

$$\beta_N = \frac{230 - K/10s}{20 \ (20 + K/10s)}, \quad K = \frac{\sqrt{2} \ \ell^4}{768EI} + \frac{3\sqrt{2} \ \ell^2}{32A_oG}$$

$$s = \frac{12 \ (1 - \nu^2)}{4 \pi Eh^3} \ \{\frac{r^2}{4} \log \frac{2r}{\ell} - \frac{3r^2}{16} + \frac{\ell^2}{16}\}$$

$$\tau_u = \frac{P}{bd}, \quad b = 2\pi (r + d)$$

ACKNOWLEDGEMENT

The author would like to acknowledge the guidance and encouragement of the late Dr. Susumu Kamiyama (Prof. of Waseda Univ.), Dr. Yuzo Akatsuka (the ex-chief, Port and Harbour Research Institute) and Dr. Yoshinori Aoki (the ex-chief, Port and Harbour Research Institute). The author wishes to thank Dr. Hajime Okamura for his helpful advice. The author is also grateful to Mr. Nobuaki Otsuki and Mr. Yoshikazu Horii for their help in the experimental work and the computation.

NOTATION

h	:	Whole height of slab (mm)
d	:	Effective height of slab (mm)
ℓ	:	Span of slab (mm)
r	:	Radius of circular loading plate (mm)
b	:	Circumference of critical section (mm)
A_o	:	Cross-sectional area of boundary beam (mm^2)
I	:	Moment inertia of boundary beam (mm^4)
ρ	:	Tensile reinforcement ratio of slab
f_{sy}	:	Yield point of reinforcing bar (MP_a)
f_c'	:	Compressive strength of concrete (MP_a)
f_{tu}	:	Tensile strength of concrete (MP_a)
E	:	Young's modulus of concrete (MP_a)
G	:	Modulus of rigidity of concrete (MP_a)
ν	:	Poisson's ratio of concrete
τ	:	Shear stress (MP_a)
τ_u	:	Shear strength (MP_a)
m_u	:	Positive ultimate resisting moment per unit width (N mm/mm)
i	:	Ratio of positive ultimate resisting moment and negative ultimate resisting moment per unit width
P	:	Concentrated load (N or KN)
P_{test}	:	Testing failure load (N or KN)
P_{flex1}	:	Ultimate flexural load in consideration of in-plane force (N or KN)
P_{flex2}	:	Ultimate flexural load due to yield line theory (N or KN)
P_{shear1}	:	Ultimate punching shear load in consideration of in-plane force (N or KN)

P_{shear2}: Ultimate punching shear load in consideration of in-plane force and influence of effective height of slab (N or KN)

K : Factor relating to rigidity of boundary beam

s : Factor relating to rigidity of slab

F_r : In-plane force of unit width acting at circumference of loading plate at the stage of flexural failure (N/mm)

w : In-plane force of unit width acting at circumference of slab at the stage of flexural failure (N/mm)

δ_c : Deflection at center of slab (mm)

$\Delta\ell_c$: Lateral movement at span center of boundary beam (mm)

Δx : Distance between neutral axis and d/2 at the stage of flexural failure (mm)

Δx_1 : Δx at circumference of loading plate (mm)

Δx_2 : Δx at circumference of slab (mm)

References

[1] Jones, L.L. et al.: Yield-line Analysis of Slabs, American Elsevier Publishing Co. Inc., 398pp., 1967.
[2] Moe, J.: Shearing strength of reinforced concrete slabs and footings under concentrated loads, Bulletin D47, PCA, 130pp., April, 1961.
[3] Yitzhaki, D.: Punching strength of reinforced concrete slabs, ACI Journal, Proc. Vol. 63, No. 5, pp. 527 to 542, May, 1966.
[4] Herzog, M.: A new evaluation of earlier punching shear tests, Concrete, Vol. 4, No. 12, pp. 448 to 450, Dec., 1970.
[5] Regan, P.: Shear in reinforced concrete-an analytical study-, Report to the CIR and IS, 199pp., April, 1971.
[6] Regan, P.: Shear in reinforced concrete-an experimental Study-, Report to the CIR and IS, 203pp., April, 1971.
[7] Kakuta, Y. et al.: Experimental study on punching strength of reinforced concrete slabs, Proc. of J.S.C.E., No. 299, pp. 105 to 115, Sept., 1974.
[8] Long. A.E.: A two-phase approach to the prediction of the punching strength of slabs, ACI Journal, Proc. Vol. 72, No. 2, pp. 37 to 45, Feb., 1975.
[9] Long, A.E. et al.: Punching failure of reinforced concrete slabs, Proc. of ICE, Vol. 37, pp. 109 to 135, May, 1967.
[10] Kinnunen, S. et al.: Punching of concrete slabs without shear reinforcement, Transactions of Swedish Royal Institute of Technology, 112pp., 1960.
[11] Ockleston, A.J.: Arching action in reinforced concrete slabs, The Structural Engineer, Vol. 36, No. 6, pp. 197 to 201, June, 1958.
[12] Hewitt, B.E.: An investigation of the punching strength of restrained slabs with particular reference to the deck slabs of composite I-beam bridges, Ph. D. Thesis, Queen's Univ., 298pp., 1972.
[13] Seki, H. et al.: Corrosion of Steel Bars at Crack of Reinforced Concrete Exposed to Sea Environments, Report of P.H.R.I., Vol. 12, No. 3, pp. 203 to 225, Sept., 1973.
[14] Kani, G.N.J.: How safe are our large reinforced concrete beams?, ACI Journal, Proc. Vol. 64, No. 3, pp. 128 to 141, March, 1967.
[15] Kennedy, R.P.: A statical analysis of the shear strength of reinforced concrete beams, Ph. D. Thesis, Stanford Univ., 256pp., 1967.
[16] Koyanagi, W.: Fracture of Concrete, Concrete Library, No. 34, pp. 93 to 111, Aug., 1972.
[17] Sub-committee on Ultimate Strength Design: Design Recommendations of Concrete Structures (2nd. Draft), J.S.C.E., 18pp., Sept., 1977.
[18] Okamura, H.: Limit State Design of Concrete Structures, Kyoritsu Publisher Ltd., 171pp., Nov., 1978.